Mean Frequency Estimation of Narrowband Signals

Kumari L. Fernando, *Member, IEEE*, V. John Mathews, *Fellow, IEEE*, and Edward B. Clark

***Abstract*—This letter shows that the single frequency approximation for a narrowband lowpass signal embedded in white noise using the Pisarenko harmonic decomposition algorithm is approximately the power-weighted mean frequency of the signal. Experimental results indicate that this method is superior to a commonly used Fourier transform based mean frequency estimation method.**

***Index Terms*—Pisarenko harmonic decomposition, power-weighted mean frequency.**

I. Introduction

In many applications, we seek to estimate the power-weighted mean frequency of a signal $x(n)$ defined as

$$\bar{\omega} = \frac{\int_{\omega_{\min}}^{\omega_{\max}} \omega P_X(\omega) d\omega}{\int_{\omega_{\min}}^{\omega_{\max}} P_X(\omega) d\omega} \tag{1}$$

where $P_X(\omega)$ is the power spectrum of $x(n)$ at the frequency ω, and $\omega_{\min}$ and $\omega_{\max}$ are respectively, the minimum and maximum frequencies of the input signal. An application of mean frequency estimation to Doppler ultrasound signal processing can be found in [1]. In current practice, the mean frequency estimation involves three steps: 1) estimate the power spectrum of the input signal, 2) evaluate the minimum and the maximum frequency values, and 3) compute the mean frequency using (1). In general, the power spectrum is estimated using a fast Fourier transform (FFT) algorithm [2], [3]. Once the spectrum is estimated, a threshold level is chosen manually such that it is larger than the noise level. The lowest and the highest frequency values at which the spectral powers equal the threshold level are selected as the minimum and the maximum signal frequencies.

In this letter, we prove that the single frequency approximation obtained using the Pisarenko harmonic decomposition (PHD) [2]–[4] for a narrowband lowpass signal embedded in white noise is approximately the power-weighted mean frequency of the signal. For the analysis, we consider signals whose bandwidth and maximum frequency are much smaller than the sampling frequency of the digitized signal. However, experimental results included in the letter show that the approximation is valid for bandwidths up to one-forth of the sampling frequency. Throughout the letter, we address this method as the PHD mean frequency estimation method. For complex-valued, narrowband signals, Miller [5] and Kasai *et al.* [6] have shown that the covariance-based frequency estimate corresponds to the power-weighted mean frequency. In [7], [8], Herment *et al.* presented an adaptive mean frequency estimator for Doppler ultrasound color flow imaging applications. However, this method depends on the assumption that the noise variance of the Doppler signal is known. No such results appear to exist for estimating power-weighted mean frequency of real-valued signals.

The rest of the letter is organized as follows. Section II contains the theoretical derivations for the PHD mean frequency estimation algorithm. Experimental results demonstrating the capabilities of the new method are presented in Section III. This section also compares the performance of our method with the conventional method in [1]. Finally, the concluding remarks are made in Section IV.

II. Mean Frequency Estimation

In this section, we first derive the algorithm for complex-valued signals. We then extend the results to the case of real-valued signals.

A. Complex-Valued Signals

Let

$$y(n) = x(n) + \eta(n) \tag{2}$$

represent the input signal, where $x(n)$ is the signal of interest and $\eta(n)$ is an additive circular white noise process with zero-mean value and variance σ_η^2. Here, $x(n)$ is a zero-mean, complex-valued narrowband signal whose bandwidth is much smaller than the sampling frequency. The covariance function $r_X(k)$ of $x(n)$ is related to its power spectrum $P_X(\omega)$ through the expression

$$r_X(k) = \frac{1}{2\pi} \int_{\omega_{\min}}^{\omega_{\max}} P_X(\omega) e^{j\omega k} d\omega \tag{3}$$

where $\omega_{\min}$ and $\omega_{\max}$ are respectively, the minimum and maximum frequencies at which the signal $x(n)$ is present. Consider the 2×2 element covariance matrix of the input signal given by

$$\mathbf{R}_Y = \begin{bmatrix} r_X(0) + \sigma_\eta^2 & r_X(1) \\ r_X^*(1) & r_X(0) + \sigma_\eta^2 \end{bmatrix} \tag{4}$$

where $r_X^*(1)$ represents the complex conjugate of $r_X(1)$. The eigenvalues of $\mathbf{R}_Y$ are

$$\lambda_1 = r_X(0) + \sigma_\eta^2 + |r_X(1)| \tag{5}$$

and

$$\lambda_2 = r_X(0) + \sigma_\eta^2 - |r_X(1)|. \tag{6}$$

Manuscript received April 10, 2003; revised June 06, 2003. This work was supported by the Primary Children's Medical Center Foundation, Salt Lake City, UT under an Innovative Research Grant. Parts of this letter were presented at the ICASSP 2002 Conference. The associate editor coordinating the review of this manuscript and approving it for publication was Prof. Zhi Ding.

K. L. Fernando and V. J. Mathews are with the Department of Electrical and Computer Engineering, University of Utah, Salt Lake City, UT 84112 USA (e-mail: fernando@eng.utah.edu).

E. B. Clark is with the Departments of Pediatrics, Bioengineering, and Obstetrics and Gynecology, University of Utah, Salt Lake City, UT 84132 USA.

Digital Object Identifier 10.1109/LSP.2003.821700

The eigenvector corresponding to the smallest eigenvalue λ_2 is

$$\mathbf{g} = m\begin{bmatrix} -\dfrac{r_X(1)}{|r_X(1)|} & 1 \end{bmatrix}^T \tag{7}$$

where m is an arbitrary constant.

We now follow the method employed in Pisarenko harmonic decomposition to estimate the frequency of a single sinusoid that best represents $\mathbf{R}_Y$. Let $\mathbf{w} = [1\ e^{j\hat{\omega}}]^H$, where $\hat{\omega}$ is the value of the single frequency that satisfies the condition $\mathbf{w}^H\mathbf{g} = 0$ and $(\cdot)^H$ denotes the Hermitian of the matrix or vector $(\cdot)$. It is straightforward to show that $\mathbf{w}^H\mathbf{g}$ can take the value of zero for an appropriate choice of $\hat{\omega}$. Substituting for $\mathbf{w}$ and $\mathbf{g}$, we get

$$\begin{bmatrix} 1 & e^{j\hat{\omega}} \end{bmatrix}\begin{bmatrix} -\dfrac{r_X(1)}{|r_X(1)|} & 1 \end{bmatrix}^T = -\frac{r_X(1)}{|r_X(1)|} + e^{j\hat{\omega}} = 0. \tag{8}$$

From (8), we can write

$$\hat{\omega} = \angle\frac{r_X(1)}{|r_X(1)|}. \tag{9}$$

As shown in [5] and [6], the frequency represented by the phase angle of the autocovariance value at lag one of a complex-valued signal is the power-weighted mean frequency of the signal. Therefore, (9) represents the power-weighted mean frequency of the input signal $x(n)$.

B. Real-Valued Signals

For real-valued signals, the covariance function $r_X(k)$ of $x(n)$ is related to the power spectrum $P_X(\omega)$ by

$$r_X(k) = \frac{1}{\pi}\int_{\omega_{\min}}^{\omega_{\max}} P_X(\omega)\cos(k\omega)d\omega \tag{10}$$

where $\omega_{\min}$ and $\omega_{\max}$ are respectively the minimum and maximum frequencies of the signal. Here, we consider the input signal $x(n)$ with both narrowband and lowpass characteristics.

Since each real-valued sinusoid can be represented by two complex-valued sinusoids, we consider 3×3 element covariance matrices. The 3×3 element covariance matrix of $y(n)$ is

$$\mathbf{R}_Y = \begin{bmatrix} r_X(0)+\sigma_\eta^2 & r_X(1) & r_X(2) \\ r_X(1) & r_X(0)+\sigma_\eta^2 & r_X(1) \\ r_X(2) & r_X(1) & r_X(0)+\sigma_\eta^2 \end{bmatrix} \tag{11}$$

and its eigenvalues are

$$\begin{aligned} \lambda_1 &= r_X(0)+\sigma_\eta^2 + \frac{1}{2}\left(r_X(2) + \sqrt{r_X^2(2)+8r_X^2(1)}\right) \\ \lambda_2 &= r_X(0)+\sigma_\eta^2 - r_X(2) \\ \lambda_3 &= r_X(0)+\sigma_\eta^2 + \frac{1}{2}\left(r_X(2) - \sqrt{r_X^2(2)+8r_X^2(1)}\right). \end{aligned}$$

We consider lowpass signals such that $|r_X(1)| > r_X(2)$.

Then, the eigenvector corresponding to the smallest eigenvalue λ_3 is

$$\mathbf{g} = m\begin{bmatrix} 1 & -\dfrac{4r_X(1)}{\sqrt{r_X^2(2)+8r_X^2(1)} - r_X(2)} & 1 \end{bmatrix}^T \tag{12}$$

where m is an arbitrary constant.

The solution to the relationship $\mathbf{w}^H\mathbf{g} = 0$, where $\mathbf{w} = [1\ e^{j\hat{\omega}}\ e^{j2\hat{\omega}}]^H$ yields

$$\cos\hat{\omega} = \frac{2r_X(1)}{\sqrt{r_X^2(2)+8r_X^2(1)} - r_X(2)}. \tag{13}$$

Substituting for $r_X^2(2)+8r_X^2(1)$ from (10) gives

$$\begin{aligned} &r_X^2(2)+8r_X^2(1) \\ &\quad= \left(\int_{\omega_{\min}}^{\omega_{\max}} P_X(\omega)\cos 2\omega d\omega\right)^2 \\ &\qquad + 8\left(\int_{\omega_{\min}}^{\omega_{\max}} P_X(\omega)\cos\omega d\omega\right)^2 \\ &\quad= \int_{\omega_{\min}}^{\omega_{\max}}\int_{\omega_{\min}}^{\omega_{\max}} P_X(\omega)P_X(\lambda)\cos 2\omega\cos 2\lambda d\omega d\lambda \\ &\qquad + 8\int_{\omega_{\min}}^{\omega_{\max}}\int_{\omega_{\min}}^{\omega_{\max}} P_X(\omega)P_X(\lambda)\cos\omega\cos\lambda d\omega d\lambda \\ &\quad= \int_{\omega_{\min}}^{\omega_{\max}}\int_{\omega_{\min}}^{\omega_{\max}} P_X(\omega)P_X(\lambda) \\ &\qquad \cdot\left((2\cos^2\omega-1)(2\cos^2\lambda-1)+8\cos\omega\cos\lambda\right)d\omega d\lambda \\ &\quad= \int_{\omega_{\min}}^{\omega_{\max}}\int_{\omega_{\min}}^{\omega_{\max}} P_X(\omega)P_X(\lambda) \\ &\qquad \cdot\left(4\cos^2\omega\cos^2\lambda - 2(\cos^2\omega+\cos^2\lambda)\right. \\ &\qquad\quad \left.+8\cos\omega\cos\lambda+1\right)d\omega d\lambda. \end{aligned} \tag{14}$$

For narrowband signals for which $(\omega_{\max} - \omega_{\min})$ is small, $(\cos\omega - \cos\lambda)^2 \approx 0$. Therefore, for $\omega_{\min} \le \omega, \lambda \le \omega_{\max}$

$$\cos^2\omega + \cos^2\lambda \approx 2\cos\omega\cos\lambda \tag{15}$$

and

$$8\cos\omega\cos\lambda - 2(\cos^2\omega+\cos^2\lambda) \approx 2(\cos^2\omega+\cos^2\lambda). \tag{16}$$

Substituting this result in (14) yields

$$r_X^2(2)+8r_X^2(1) \approx \left[\int_{\omega_{\min}}^{\omega_{\max}} P_X(\omega)(2\cos^2\omega+1)d\omega\right]^2. \tag{17}$$

Applying this result to (13) gives

$$\cos\hat{\omega} \approx \frac{\int_{\omega_{\min}}^{\omega_{\max}} P_X(\omega)\cos\omega d\omega}{\int_{\omega_{\min}}^{\omega_{\max}} P_X(\omega)d\omega}. \tag{18}$$

That is,

$$\cos\hat{\omega}\int_{\omega_{\min}}^{\omega_{\max}} P_X(\omega)d\omega \approx \int_{\omega_{\min}}^{\omega_{\max}} P_X(\omega)\cos\omega d\omega. \tag{19}$$

Dividing both sides of (19) by $\cos\hat{\omega}$ results in

$$\int_{\omega_{\min}}^{\omega_{\max}} P_X(\omega)d\omega \approx \int_{\omega_{\min}}^{\omega_{\max}} P_X(\omega)\frac{\cos\omega}{\cos\hat{\omega}}d\omega. \tag{20}$$

Multiply both the numerator and the denominator with $\sin\hat{\omega}$ gives

$$\int_{\omega_{\min}}^{\omega_{\max}} P_X(\omega)d\omega \approx \int_{\omega_{\min}}^{\omega_{\max}} P_X(\omega)\frac{\cos\omega\sin\hat{\omega}}{\cos\hat{\omega}\sin\hat{\omega}}d\omega. \tag{21}$$

Since $(\omega_{\max}-\omega_{\min})$ is small and $\omega_{\min} \le \omega \le \omega_{\max}$, $(\omega+\hat{\omega}) \approx 2\hat{\omega}$ and $\sin(\omega-\hat{\omega}) \approx (\omega-\hat{\omega})$. Therefore,

$$\begin{aligned}\frac{\cos\omega\sin\hat{\omega}}{\cos\hat{\omega}\sin\hat{\omega}} &= \frac{0.5\sin(\omega+\hat{\omega})-0.5\sin(\omega-\hat{\omega})}{0.5\sin 2\hat{\omega}} \\ &\approx 1-\frac{\omega-\hat{\omega}}{\sin 2\hat{\omega}}.\end{aligned} \tag{22}$$

Substituting this result in (20) gives

$$\int_{\omega_{\min}}^{\omega_{\max}} P_X(\omega)d\omega \approx \int_{\omega_{\min}}^{\omega_{\max}} P_X(\omega)\left[1-\frac{\omega-\hat{\omega}}{\sin 2\hat{\omega}}\right]d\omega \tag{23}$$

implying that

$$\int_{\omega_{\min}}^{\omega_{\max}} P_X(\omega)\frac{(\omega-\hat{\omega})}{\sin 2\hat{\omega}}d\omega \approx 0. \tag{24}$$

Since $\sin 2\hat{\omega} \neq 0$, solving (24) for $\hat{\omega}$ yields

$$\hat{\omega} \approx \frac{\int_{\omega_{\min}}^{\omega_{\max}} P_X(\omega)\omega d\omega}{\int_{\omega_{\min}}^{\omega_{\max}} P_X(\omega)d\omega}. \tag{25}$$

According to the above derivation, the single frequency estimation for a real-valued narrowband lowpass signal using the eigendecomposition of the 3×3 element covariance matrix is approximately equal to the power-weighted mean frequency of the signal.

III. Experimental Results

In this section, we present the results of several experiments using the simulated narrowband signals. For these experiments, a narrowband signal was generated with its spectrum given by

$$P_X(\omega) = \begin{cases} \frac{1}{\sqrt{\sigma_\omega^2}}e^{-\frac{(\omega-\omega_m)^2}{2\sigma_\omega^2}}, & \omega_{\min} \le \omega \le \omega_{\max} \\ 0, & \text{otherwise} \end{cases} \tag{26}$$

where ω_m and σ_ω were constant parameters of the model. The signal was then corrupted by additive white, Gaussian noise with zero mean value and variance σ_η^2. The sampling frequency was 12 000 samples/sec, $\sigma_\omega = 600\pi$ rad/s, $\omega_m = 3000\pi$ rad/s, $\omega_{\min} = 2400\pi$ rad/s, and $\omega_{\max} = 4500\pi$ rad/s. The power-weighted mean frequency and the bandwidth of the signal were $\bar{\omega} = 3161.2\pi$ rad/s and 2100π rad/s, respectively.

The mean frequency was estimated from 512 samples of the data and 1000 independent experiments were performed at ten different SNR values between -5 and 30 dB. The normalized root-mean-square (rms) error σ_e was estimated as

$$\sigma_e = \frac{\sqrt{\frac{1}{1000}\sum_{i=1}^{1000}|\hat{\omega}_i-\bar{\omega}|^2}}{\bar{\omega}} \tag{27}$$

where $\hat{\omega}_i$ was the frequency estimate for the ith experiment.

The results obtained as above were also compared with direct measurement of the power-weighted mean frequency using the FFT-based method. First, power spectrum of the Hann-windowed input signal was estimated using the periodogram method. The FFT-size was 1024 samples. Then, a threshold value was manually chosen such that it is above the noise level of the spectrum and provided the minimum rms error σ_e. The minimum and the maximum frequency values of the spectrum were estimated such that they were the minimum and the maximum frequency values at which the estimated spectrum crossed the threshold. The mean frequency values were then estimated using

$$\hat{\omega} = \frac{\sum_{\omega=\omega_{\min}}^{\omega_{\max}} \omega\hat{P}_X(\omega)}{\sum_{\omega=\omega_{\min}}^{\omega_{\max}} \hat{P}_X(\omega)} \tag{28}$$

where $\hat{P}_X(\omega)$ was the estimated power spectrum.

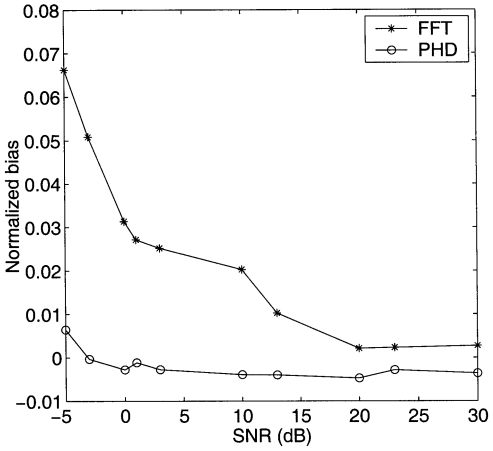

Fig. 1. Distribution of the normalized bias with the SNR for the PHD mean frequency estimation method and the conventional FFT-based method for real-valued narrowband signals.

Figs. 1 and 2 show the variation of the normalized bias and the rms error, respectively for several SNR values from -5 to 30 dB for these two algorithms. As can be seen from Fig. 1, the estimated mean frequency values exhibit only a slight bias for the PHD method whereas the FFT-based method exhibits a larger bias. In addition, Fig. 2 demonstrates that the PHD method exhibits smaller variability in the estimates than the FFT-based approach. The variation of the normalized rms error for the PHD method is relatively small with the SNR values above 0 dB.

Fig. 3 demonstrates the robustness of the algorithm against the assumption that bandwidth of the signal is much smaller than the sampling frequency. According to the figure, the variability increases with the bandwidth of the signal. This result is to be

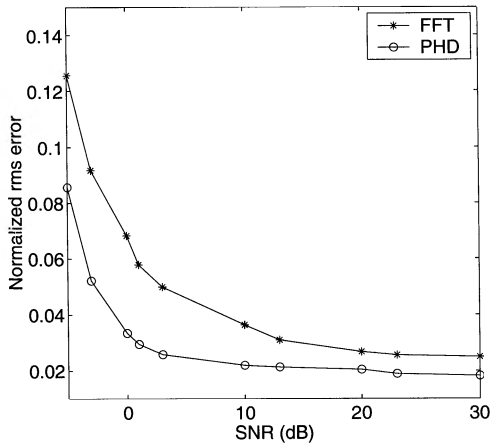

Fig. 2. Distribution of the rms error with the SNR for the PHD mean frequency estimation method and the conventional FFT-based method for real-valued narrowband signals.

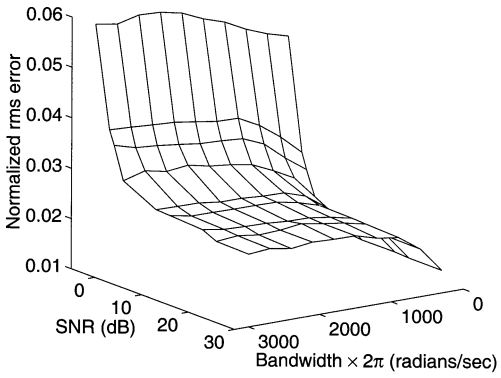

Fig. 3. Distribution of the rms error for the PHD mean frequency estimation method with the SNR and the bandwidth.

expected, since the narrowband-approximation employed in the derivations become less accurate with the increase in bandwidth of the input signal. In spite of this, it is interesting to note that the rms errors for SNR above 0 dB are less than 3% of the true mean frequency value even for a signal bandwidth of one-forth of the sampling frequency. For comparison, we also evaluated the performance of the FFT-based method with the variation of both the SNR and the bandwidth of the signal. The results are depicted in Fig. 4. The rms estimation error is larger than that for the PHD method for all the cases. These results indicate that the estimation of mean frequencies for real-valued signals using the PHD mean frequency estimation method outperforms the conventional FFT-based method.

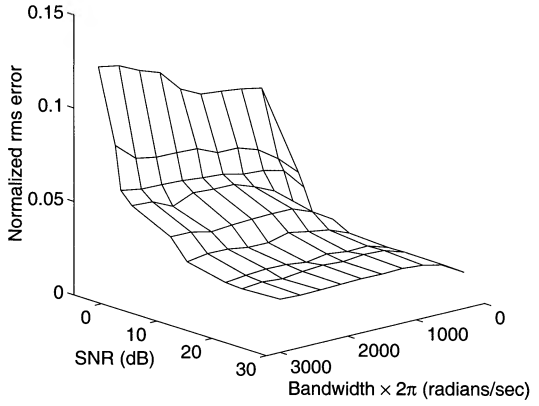

Fig. 4. Distribution of the rms error for the FFT-based mean frequency estimation method with the SNR and the bandwidth.

IV. Concluding Remarks

This letter presented an algorithm to estimate the power-weighted mean frequency of narrowband lowpass signals using the Pisarenko harmonic decomposition of the covariance matrix of the input data. Experimental results indicate that this method is relatively unbiased and provides accurate results for SNRs above 0 dB. An application of this approach for the reconstruction of mean blood velocity waveforms from Doppler ultrasound measurements is described in [9].

References

[1] N. T. C. Ursem, H. J. F. Brinkman, P. C. Struijk, W. C. J. Hop, M. H. Kempski, B. K. Keller, and J. W. Wladimiroff, "Umbilical artery waveform analysis based on maximum, mean, and mode velocity in early human pregnancy," *Ultrasound Med. Biol.*, vol. 24, no. 1, pp. 1–7, 1998.

[2] P. Stoica and R. Moses, *Introduction to Spectral Analysis*. Upper Saddle River, NJ: Prentice-Hall, 1997.

[3] S. M. Kay, *Modern Spectral Estimation*. Englewood Cliffs, NJ: Prentice-Hall, 1988.

[4] V. F. Pisarenko, "The retrieval of harmonics from a covariance function," *Geophys. J. R. Astron. Soc.*, vol. 33, pp. 347–366, 1973.

[5] K. S. Miller, "A covariance approach to spectral moment estimation," *IEEE Trans. Inform. Theory*, vol. 18, no. 5, pp. 588–596, 1972.

[6] C. Kasai, K. Namekawa, A. Koyano, and R. Omoto, "Real-time two-dimensional blood flow imaging using an autocorrelation technique," *IEEE Trans. Sonics Ultrasonics*, vol. 32, pp. 458–463, Mar. 1985.

[7] A. Herment, G. Demoment, P. Dumee, J. P. Guglielmi, and A. Delouche, "A new adaptive mean frequency estimator: application to constant variance color flow mapping," *IEEE Trans. Ultrasonics, Ferroelectron., Frequency Control*, vol. 40, pp. 796–804, June 1993.

[8] A. Herment, G. Demoment, and P. Dumee, "Improved estimation of low velocities in color Doppler imaging by adapting the mean frequency estimator to the clutter rejection filter," *IEEE Trans. Biomed. Eng.*, vol. 43, pp. 919–927, Sept. 1996.

[9] K. L. Fernando, V. J. Mathews, and E. B. Clark, "Mean frequency estimation of narrowband signals and its application to Doppler ultrasound blood velocity waveform estimation," in *Proc. IEEE Int. Conf. Acoustics, Speech, Signal Processing* Orlando, FL, May 2002, vol. 2, pp. 1317–1320.